GPS Solutions (2021) 25:129
https://doi.org/10.1007/s10291-021-01162-7

ORIGINAL ARTICLE

Broadcast ephemerides for LEO augmentation satellites based on nonsingular elements

Lingdong Meng[1,2] · Junping Chen[2,3] · Jiexian Wang[1] · Yize Zhang[2]

Received: 9 November 2020 / Accepted: 3 July 2021

Abstract

Low earth orbit (LEO) satellite constellations have the potential to augment global navigation satellite system services. Among the ongoing tasks of LEO-based navigation, providing broadcast ephemerides that satisfy the accuracy requirement for positioning, navigation, and timing is one of the most critical prerequisites. Singularities can occur when fitting broadcast ephemeris parameters in the case of a small eccentricity or small or large inclination. We choose an improved nonsingular element set for the LEO broadcast ephemeris design. We establish suitable broadcast ephemeris models, considering the fit accuracy, number of parameters, orbital altitude, and inclination. The fit accuracy using different orbital altitudes, orbital inclinations, and eccentricities suggests that the optimal parameters are $\dot{n}$, $\ddot{n}$, C_{rc3}, C_{rs3}, $C_{\lambda c3}$, and $C_{\lambda s3}$, together with the basic broadcast ephemeris model. After adding these six parameters, a fit accuracy of better than 10 cm can be achieved with a 20 min arc length and 500–1400 km orbital altitudes. The effects of the number of parameters, orbital altitude, inclination, and eccentricity on the fit accuracy are discussed in detail. Finally, the performance is validated with real LEO satellites to confirm the effectiveness of the proposed method.

Keywords Nonsingular orbital elements set · LEO navigation augmentation · Kepler ephemeris model · Broadcast ephemeris

Introduction

Current global navigation satellite systems (GNSSs), such as the Global Positioning System (GPS), the Global Navigation Satellite System (GLONASS), Galileo, and BeiDou use satellites located in medium earth orbits (MEOs). In addition, the BeiDou system includes geostationary equatorial orbits (GEOs), and inclined geosynchronous orbits (IGSOs). However, low earth orbit (LEO) satellites have not yet been used to provide positioning, navigation, and timing (PNT) services.

Currently, multi-GNSS with LEO constellation augmentation has become a research topic of much interest. Companies such as SpaceX, Orbcomm, and Globalstar have tried to establish commercial broadband LEO satellite constellations to deliver Internet services globally. They can also provide services such as navigation systems do (Reid et al. 2016). Although approximately 120 GNSS satellites are available (Li et al. 2015), weak signals are a challenge for many GNSS constellations, whereas the LEO satellites can deliver strong signals for users due to the low orbital altitudes (Enge et al. 2012). Benefiting from the fast motion of LEO satellites, large geometric variations can be achieved, thereby accelerating the convergence of precise point positioning (PPP) (Joerger et al. 2010; Li et al. 2019a). Therefore, introducing LEO constellations into current GNSSs will benefit PNT services (Li et al. 2019b). However, the reliability of the broadcast ephemeris is one of the key problems for constructing multi-GNSS augmented by an LEO constellation.

Generally, broadcast parameters are calculated via a least-square or QR factorization curve fit of the predicted precise ephemeris (Montenbruck and Gill 2000). Legacy navigation (LNAV) and civil navigation (CNAV) messages

✉ Junping Chen
junping@shao.ac.cn

[1] College of Surveying and Geo-Informatics, Tongji University, Shanghai 200092, People's Republic of China

[2] Shanghai Astronomical Observatory, Chinese Academy of Sciences, Shanghai 200030, People's Republic of China

[3] School of Astronomy and Space Science, University of Chinese Academy of Sciences, Beijing 100049, People's Republic of China

Published online: 22 July 2021

(Steigenberger et al. 2015; Wang et al. 2019) are designed based on Kepler orbit elements, which are used in the GPS, Galileo, and BeiDou constellations (CSNO 2013; EU 2015; GPS Directorate 2013). A MEO is defined by 16 or 18 parameters in LNAV or CNAV broadcast ephemeris models. Compared with LNAV, the CNAV can achieve high-accuracy orbital representations (Yin et al. 2015). In contrast to the GNSSs mentioned above, the Cartesian ephemeris model is used in GLONASS (ICD-GLONASS 2016), and numerical integration is used to compute the GLONASS satellite position, which may be complicated for users. The performance of broadcast ephemeris data is affected mainly by model fit errors, orbit determination, and propagation errors. Around 2014, the only orbital contributions to the user range error (URE) were approximately 0.24, 0.54, 0.76, and 0.57 m for the GPS, GLONASS, Galileo, and BeiDou IGSO and MEO satellites, respectively (Montenbruck et al. 2015).

Broadcast ephemeris design has focused mainly on MEO, IGSO, or GEO satellites. In constructing LEO-constellation-augmented multi-GNSSs, the design of broadcast ephemeris parameters is an essential issue. Unlike MEO, IGSO, and GEO satellites, LEO satellites are close to the earth and are seriously affected by higher-order gravity and atmospheric conditions. Therefore, LNAV and CNAV broadcast ephemeris models cannot describe the complex orbital dynamics for LEO satellites. The Kepler ephemeris model and some nonsingular element sets may be singular in some cases. For Kepler orbital elements, the argument of perigee, for example, is not a useful orbital element in the case of small eccentricities. Therefore, an improved nonsingular element set has been proposed in Montenbruck and Gill (2000), considering nonsingular characteristics. In recent years, researchers have proposed a trade-off strategy to solve the singularity caused by a small inclination (Ruan et al. 2011). In their strategy, the orbit of a GEO satellite is regarded as the pseudo-GEO satellite by intentionally adding 5° to the original small inclination. Once users receive the ephemeris parameters, users have to rotate back 5° to obtain the correct GEO satellite positions. Although the singularity caused by a small inclination can be removed to some degree, the algorithm for parameter fitting and satellite position computation is complicated. Xie et al. (2018) used another nonsingular element set to remove the singularity caused by a small eccentricity. However, the singularity caused by small inclinations cannot be removed. When the orbital inclination is close to zero, the right ascension of the ascending node (RAAN) is not well defined. Choi et al. (2020) attempted to remove this singularity by intentionally adding 5° to the original small inclination. However, the fit accuracy of satellites with small inclinations using this strategy is always worse than that of other satellites. Another nonsingular element set suitable for GEO satellites was introduced to remove the singularities caused by small eccentricity and inclination (Du et al. 2014). However, when the inclination is close to 90°, singularities remain.

As mentioned above, not all singularities can be removed simultaneously. We introduce an improved nonsingular element set that can overcome the drawbacks of the nonsingular element sets used by Du et al. (2014) and Xie et al. (2018). To reduce the fit errors of LEO satellites, a few additional parameters are considered. In the following, we first present the improved nonsingular element set for LEO satellites; then, the fit accuracy and parameter selections are revealed. Next, the influences of the arc length, orbital altitude, inclination, and eccentricity on the fit accuracy are discussed. Finally, the performance of the proposed broadcast ephemeris model is verified using real LEO satellites.

Improved nonsingular elements for LEO

Kepler elements $(a, e, i, \Omega, \omega, M)$ are widely used to describe satellite motion in GNSSs. These parameters denote the semimajor axis, eccentricity, inclination, RAAN, argument of perigee, and mean anomaly.

However, in many applications, satellite orbits are nearly circular. For some satellites, the inclination is very close to zero. Although the satellite position can still be calculated correctly when e and i are close to zero, the reverse task may cause practical and numerical problems when Kepler elements or some nonsingular element sets are used. In theory, this phenomenon is caused by singularities arising from the definition of some orbital elements. LEO satellites with small eccentricities and small or large inclinations may be used in the future construction of LEO navigation systems (Ma et al. 2020). Therefore, nonsingular elements have been applied to remove singularities (Du et al. 2014; Xie et al. 2018). However, as noted above, the nonsingular element sets previously studied have only partly removed singularities. An improved nonsingular element set $\left(A, e_x, e_y, i_x, i_y, M^*\right)$ is used in this study for the design of LEO broadcast ephemeris to remove singularities. This set of elements, which is suitable for orbits with small eccentricities and small or large inclinations, is defined by

$$\begin{cases} A, \boldsymbol{e} = (e_x,\ e_y)^T = (e\cos\tilde{\omega}, e\sin\tilde{\omega})^T \\ \boldsymbol{i} = (i_x, i_y) = (\sin\frac{i}{2}\cos\Omega, \sin\frac{i}{2}\sin\Omega)^T,\ M^* = \Omega + \omega + M \end{cases} \tag{1}$$

where A is the semimajor axis and $\boldsymbol{e}$ and $\boldsymbol{i}$ are the eccentricity and inclination vectors, respectively. $M*$ denotes the mean longitude, and $\tilde{\omega}$ can be defined by

$$\tilde{\omega} = \Omega + \omega \tag{2}$$

The fast mean motion M^* angular variable is then measured from the vernal equinox. Furthermore, the definition of the inclination vector is modified from that of the nonsingular element set used by Du et al. (2014).

The central force of the earth is the major driver of satellites. Other forces, such as atmospheric drag and luni-solar attractions, cause complex perturbations. Compared with MEO satellites, LEO satellites are easily influenced by atmospheric drag. The effect of these forces on nonsingular elements can be classified into short-periodic, long-periodic, and secular variations (Xie et al.2018).

Basic broadcast ephemeris model based on the improved nonsingular element set

In addition to the improved nonsingular elements, extra parameters are needed to represent short-periodic, long-periodic, and secular variations. Referring to GPS LNAV ephemerides, nine additional correction terms are included to compensate for the dominant perturbation forces and the variations in orbital elements. The algorithm for the basic broadcast model is then discussed. Finally, the strategy of broadcast ephemeris generation is briefly introduced.

Basic broadcast ephemeris model

Similar to the GPS LNAV message, six second-order harmonic correction terms $\left(C_{rc}, C_{rs}, C_{\lambda c}, C_{\lambda s}, C_{Nc}, C_{Ns}\right)$ are included to account for the short-periodic variations with a period equivalent to half a revolution. Furthermore, three rate terms $\left(\Delta n, \dot{i}_x, \dot{i}_y\right)$ are used to describe secular and long-periodic variations. The specific meanings of the basic parameters are provided in Table 1.

User algorithm

Satellite positions can be calculated using the basic broadcast ephemeris model: the computation process is similar to the process used for LANV. The detailed calculation process for the satellite position at epoch t is as follows:

$$t_k = t - t_{\mathrm{oe}} \tag{3}$$

$$A_k = A_{\mathrm{ref}} + \Delta A \tag{4}$$

$$n = \sqrt{\frac{\mathrm{GM}}{A_k^3}} \tag{5}$$

where A_{ref} is the reference value of the semimajor axis, GM is the gravitational constant of the earth, and t_{oe} is the reference epoch.

The mean longitude M^* can be obtained by

$$M^* = M_0^* + (n + \Delta n)t_k \tag{6}$$

The generalized Kepler equation is then used to calculate the eccentric longitude E^*

$$E^* - e_x \sin E^* + e_y \cos E^* = M^* \tag{7}$$

Then, the true longitudes f_0^* can be obtained by

$$f_0^* = \arctan\left(\frac{\sin f_0^*}{\cos f_0^*}\right) \tag{8}$$

where $\sin f_0^*$ and $\cos f_0^*$ can be computed as follows:

$$\sin f_0^* = \frac{A_k}{r_o}\left(\sin E^* - e_y + \frac{e_x}{\beta}\left(-e_x \sin E^* + e_y \cos E^*\right)\right) \tag{9}$$

$$\cos f_0^* = \frac{A_k}{r_o}\left(\cos E^* - e_x - \frac{e_y}{\beta}\left(-e_x \sin E^* + e_y \cos E^*\right)\right) \tag{10}$$

where $r_0 = A_k\left(1 - e_x \cos E^* - e_y \sin E^*\right)$ and $\beta = 1 + \sqrt{1 - \left(e_x^2 + e_y^2\right)}$.

The three components in the radial, along-track, and cross-track directions, considering their respective short-period corrections, can be calculated as follows

$$\begin{aligned} r &= r_0 + \delta r \\ &= r_0 + C_{\mathrm{rc}} \cos 2f_0^* + C_{\mathrm{rs}} \sin 2f_0^* \end{aligned} \tag{11}$$

$$\begin{aligned} f^* &= f_0^* + \delta f_0^* \\ &= f_0^* + C_{\lambda c} \cos f_0^* + C_{\lambda s} \sin f_0^* \end{aligned} \tag{12}$$

$$N = C_{\mathrm{Nc}} \cos 2f_0^* + C_{\mathrm{Ns}} \sin 2f_0^* \tag{13}$$

Next, the satellite position in the orbital plane coordinate system is

Table 1 Parameters of the basic broadcast ephemeris model

Parameter	Meaning
ΔA	Semimajor axis difference from the reference value
e_x, e_y	Components of eccentricity vector
i_{x0}, i_{y0}	Components of inclination vector
M_0^*	Mean longitude
Δn	Mean motion difference from the calculated value
$\dot{i}_x$, $\dot{i}_y$	Rates of inclination vector components
C_{rc}, C_{rs}	Correction coefficients of geocentric distance
$C_{\lambda c}$, $C_{\lambda s}$	Correction coefficients of true longitude
C_{Nc}, C_{Ns}	Correction coefficients of out-of-plane distance

$$\mathbf{r} = \begin{pmatrix} r\cos f^* \\ r\sin f^* \\ N \end{pmatrix} \tag{14}$$

The satellite position coordinates in the orbital plane are rotated into the earth-centered inertial (ECI) coordinate system using transformation matrix $\boldsymbol{M}$

$$\boldsymbol{M} = \begin{pmatrix} 1-2i_y^2 2i_x i_y - 2i_y\sqrt{1-\left(i_y^2+i_x^2\right)} \\ 2i_x i_y 1-2i_y^2 2i_x\sqrt{1-\left(i_y^2+i_x^2\right)} \\ 2i_y\sqrt{1-\left(i_y^2+i_x^2\right)} - 2i_x\sqrt{1-\left(i_y^2+i_x^2\right)}\cos i \end{pmatrix} \tag{15}$$

where

$$i_x = i_{x0} + \dot{i}_x t_k \tag{16}$$

$$i_y = i_{y0} + \dot{i}_y t_k \tag{17}$$

$$\cos i = 1 - 2\left(i_x^2 + i_y^2\right) \tag{18}$$

Finally, the ECI coordinates can be transformed into the earth-centered earth-fixed (ECEF) coordinate system using transformation matrix $R_z\left(\theta_g\right)$ and

$$\theta g = \omega_e\left(t - t_{\mathrm{oe}}\right) \tag{19}$$

where ω_e is the mean rotation velocity of the earth and θ_g is the Greenwich sidereal time angle after time t_{oe}.

The process above for users is similar to that of LNAV or CNAV ephemerides. Therefore, the computational complexity is acceptable.

Parameter fitting

For parameter fitting, two problems should be carefully considered: how to estimate the parameters and how to calculate partial derivatives for each parameter. Generally, the broadcast ephemeris parameters are fitted by least squares. However, the normal equations are ill-conditioned in some cases and are extremely sensitive to small errors in the normal equation matrix. Therefore, a different treatment of the least-squares problem based on QR factorization is recommended (Montenbruck and Gill 2000).

When broadcast ephemeris parameters are generated, the partial derivatives of each parameter should be calculated. Unfortunately, the structure of the partial derivatives is usually complex. The corresponding formulas are laborious and prone to errors. By contrast, the numerical derivative method used to calculate the partial derivatives of orbital elements is convenient and straightforward. The numerical derivative method has been successfully applied in fitting GPS broadcast parameters (Wang and Wang 2014). Therefore, we use the numerical derivative method to calculate partial derivatives and QR factorization for parameter fitting to fit the broadcast parameters. Thus, laborious partial derivatives can be avoided, and more reliable numerical stability can be achieved.

LEO broadcast ephemeris parameter design

The 16-parameter basic broadcast ephemeris model cannot satisfy the accuracy demand for LEO satellites. Extra parameters are introduced into the basic ephemeris model. Considering the variation characteristics of the orbital elements, first-order and third-order harmonic parameters $(C_{rc1}, C_{rs1}, C_{rc3}, C_{rs3}, C_{\lambda c1}, C_{\lambda s1}, C_{\lambda c3}, C_{\lambda s3}, C_{Nc1}, C_{Ns1}, C_{Nc3}, C_{Ns3})$ might be added to account for the short-period variations. Then, the short-periodic corrections in the radial, along-track, and cross-track directions can be computed as

$$\delta r = C_{rc1}\cos f_0^* + C_{rs1}\sin f_0^* + C_{rc}\cos 2f_0^* + C_{rs}\sin 2f_0^* + C_{rc3}\cos 3f_0^* + C_{rs3}\sin 3f_0^* \tag{20}$$

$$\delta f_0^* = C_{\lambda c1}\cos f_0^* + C_{\lambda s1}\sin f_0^* + C_{\lambda c}\cos 2f_0^* + C_{\lambda s}\sin 2f_0^* + C_{\lambda c3}\cos 3f_0^* + C_{\lambda s3}\sin 3f_0^* \tag{21}$$

$$N = C_{Nc1}\cos f_0^* + C_{Ns1}\sin f_0^* + C_{Nc}\cos 2f_0^* + C_{Ns}\sin 2f_0^* + C_{Nc3}\cos 3f_0^* + C_{Ns3}\sin 3f_0^* \tag{22}$$

In addition, second-order rates $\left(\dot{A}, \ddot{A}, \dot{n}, \ddot{n}, \ddot{i}_x, \ddot{i}_y\right)$ of the semimajor axis, mean motion, and inclination vector may also be possible options for describing in depth the secular and long-periodic variations. They can be computed as

$$A_k = A_{\mathrm{ref}} + \Delta A + \dot{A}t_k + \frac{1}{2}\ddot{A}t_k^2 \tag{23}$$

$$n = \sqrt{\frac{\mathrm{GM}}{A_k^3}} + \Delta n + \dot{n}t_k + \frac{1}{2}\ddot{n}t_k^2 \tag{24}$$

$$i_x = i_{x0} + \dot{i}_x t_k + \frac{1}{2}\ddot{i}_x t_k^2 \tag{25}$$

$$i_y = i_{y0} + \dot{i}_y t_k + \frac{1}{2}\ddot{i}_y t_k^2 \tag{26}$$

After some of these optional parameters are added, the satellite motion can be described more precisely, and the fit accuracy can be improved.

Results

The performance of several broadcast ephemeris designs for LEO satellites is assessed considering some parameters of high-order rates and first- and third-order harmonic parameters. Then, the performance of broadcast ephemeris designs is evaluated.

Elevation fitting accuracy index

The orbit errors Δr can be divided into the radial (ΔR), along-track (ΔA), and cross-track (ΔC) directions. The URE is an important index that reflects the impact of Δr on the user line-of-sight vector. The fit errors should be no more than 10 cm (Department 2008). The orbit-only contribution to the URE is defined as a weighted average of RMS errors $A = \mathrm{RMS}(\Delta A)$, $C = \mathrm{RMS}(\Delta C)$, and $R = \mathrm{RMS}(\Delta R)$, as follows:

$$\mathrm{URE} = \sqrt{w_R^2 R^2 + w_{A,C}^2 \left(A^2 + C^2\right)} \tag{27}$$

The weight factors w_R and $w_{A,C}$ are positively related to the orbital altitude. The values of the weight factors for LEO satellites range from 400 to 1400 km and are listed in Table 2. For LEO satellites, the contributions of the cross-track and along-track directions are much more significant. Therefore, parameters that describe cross-track and along-track variation should be added.

Table 2 User range error (URE) weight factors for different orbital altitude low earth orbit (LEO) satellites (Xie et al. 2018)

Orbital altitude (km)	w_R	$w_{A,C}$
400	0.419	0.642
600	0.488	0.617
800	0.540	0.595
1000	0.582	0.575
1200	0.618	0.556
1400	0.648	0.539

Fit accuracy of different designs

In this study, we consider only the model fit errors, which the URE reflects. The satellite orbits are simulated using Satellite Tool Kit (STK) software (Li et al. 2019b). The eccentricity and inclination of the orbits used in Tables 3, 4, 5 and 6 are 0.001 and 0° or 45°, and the uniform data sample rate is 60 s.

We use the basic broadcast ephemeris model to fit precise orbits of 1000 km and 800 km altitudes. As shown in Table 3, the average 20 min fit errors are 0.888, 0.888 and 0.013 m in the radial (R), along-track (A), and cross-track (C) components, respectively. When the arc length increases to 30 min, the average errors increase substantially to 4.835, 4.862, and 0.071 m in the three directions, respectively, as shown in Table 4. Similar results are presented in Tables 5 and 6. The fit errors in the cross-track direction are much smaller than those in the radial and along-track directions.

Table 3 Results of fit errors in the radial (R), along-track (A) and cross-track (C) components and URE values with a 20 min arc length for the 1000 km LEO satellite (unit: m)

No. parameters	Extra parameters	URE RMS	R	A	C	Inclination (°)
16		0.727	0.888	0.888	0.013	0
17	$\dot{A}$	0.098	0.120	0.120	0.013	0
	$\dot{n}$	0.092	0.112	0.112	0.013	0
18	C_{rc3}, C_{rs3}	0.149	0.182	0.183	0.013	0
	$\dot{A}$, $\dot{n}$	0.082	0.100	0.100	0.013	0
	$\dot{A}$, $\ddot{A}$	0.063	0.077	0.076	0.013	0
	$\dot{n}$, $\ddot{n}$	0.047	0.057	0.057	0.013	0
19	$\dot{n}$, C_{rc3}, C_{rs3}	0.037	0.044	0.044	0.013	0
	$\dot{A}$, C_{rc3}, C_{rs3}	0.035	0.041	0.042	0.013	0
	$\dot{A}$, $\ddot{A}$,$\dot{n}$	0.026	0.031	0.031	0.013	0
	$\dot{A}$, $\dot{n}$,$\ddot{n}$	0.025	0.029	0.029	0.013	0
20	C_{rc3}, C_{rs3}, $C_{\lambda c3}$,$C_{\lambda s3}$	0.024	0.027	0.027	0.013	0
	$\dot{n}$, $\ddot{n}$, C_{rc3}, C_{rs3}	0.020	0.022	0.022	0.013	0
	$\dot{A}$, $\ddot{A}$, C_{rc3}, C_{rs3}	0.019	0.021	0.022	0.013	0
21	$\dot{A}$, C_{rc3}, C_{rs3}, $C_{\lambda c3}$,$C_{\lambda s3}$	0.013	0.014	0.013	0.013	0
	$\dot{n}$, C_{rc3}, C_{rs3}, $C_{\lambda c3}$,$C_{\lambda s3}$	0.013	0.013	0.013	0.013	0
22	$\dot{n}$, $\ddot{n}$, C_{rc3}, C_{rs3}, $C_{\lambda c3}$,$C_{\lambda s3}$	**0.012**	**0.011**	**0.012**	**0.013**	0

Table 4 Results of fit errors in the radial (R), along-track (A), and cross-track (C) components and URE values with a 30 min arc length for the1000 km LEO satellite (unit: m)

No. parameters	Extra parameters	URE RMS	R	A	C	Inclination (°)
16		3.967	4.835	4.862	0.071	0
17	$\dot{A}$	0.679	0.830	0.827	0.069	0
	$\dot{n}$	0.633	0.773	0.772	0.069	0
18	C_{rc3}, C_{rs3}	1.095	1.336	1.338	0.069	0
	$\dot{A}$, $\dot{n}$	0.571	0.698	0.695	0.069	0
	$\dot{A}$, $\ddot{A}$	0.379	0.460	0.461	0.069	0
	$\dot{n}$, $\ddot{n}$	0.192	0.229	0.230	0.069	0
19	$\dot{n}$, C_{rc3}, C_{rs3}	0.369	0.448	0.449	0.069	0
	$\dot{A}$, C_{rc3}, C_{rs3}	0.326	0.395	0.396	0.069	0
	$\dot{A}$, $\ddot{A}$,$\dot{n}$	0.141	0.164	0.166	0.069	0
	$\dot{A}$, $\dot{n}$,$\ddot{n}$	0.125	0.144	0.146	0.069	0
20	C_{rc3}, C_{rs3}, $C_{\lambda c3}$,$C_{\lambda s3}$	0.208	0.247	0.252	0.069	0
	$\dot{n}$, $\ddot{n}$, C_{rc3}, C_{rs3}	0.101	0.113	0.113	0.069	0
	$\dot{A}$, $\ddot{A}$, C_{rc3}, C_{rs3}	0.097	0.108	0.107	0.069	0
21	$\dot{A}$, C_{rc3}, C_{rs3}, $C_{\lambda c3}$,$C_{\lambda s3}$	0.068	0.068	0.068	0.069	0
	$\dot{n}$, C_{rc3}, C_{rs3}, $C_{\lambda c3}$,$C_{\lambda s3}$	0.067	0.066	0.066	0.069	0
22	$\dot{n}$,$\ddot{n}$, C_{rc3}, C_{rs3}, $C_{\lambda c3}$,$C_{\lambda s3}$	**0.058**	**0.052**	**0.052**	**0.069**	0

Table 5 Results of fit errors in the radial (R), along-track (A), and cross-track (C) components and URE values with a 20 min arc length for the 800 km LEO satellite (unit: m)

No. parameters	Extra parameters	URE RMS	R	A	C	Inclination (°)
16		3.401	3.322	3.367	3.499	45
17	$\dot{A}$	0.381	0.399	0.400	0.344	45
	$\dot{n}$	0.352	0.365	0.367	0.326	45
18	C_{rc3}, C_{rs3}	0.707	0.708	0.716	0.697	45
	$\dot{A}$, $\dot{n}$	0.357	0.374	0.376	0.322	45
	$\dot{A}$, $\ddot{A}$	0.187	0.187	0.188	0.186	45
	$\dot{n}$, $\ddot{n}$	0.061	0.062	0.065	0.054	45
19	$\dot{n}$, C_{rc3}, C_{rs3}	0.155	0.161	0.161	0.143	45
	$\dot{A}$, C_{rc3}, C_{rs3}	0.144	0.151	0.151	0.131	45
	$\dot{A}$, $\ddot{A}$,$\dot{n}$	0.049	0.048	0.051	0.048	45
	$\dot{A}$, $\dot{n}$,$\ddot{n}$	0.043	0.043	0.045	0.040	45
20	C_{rc3}, C_{rs3}, $C_{\lambda c3}$,$C_{\lambda s3}$	0.077	0.075	0.078	0.078	45
	$\dot{n}$, $\ddot{n}$, C_{rc3}, C_{rs3}	0.034	0.034	0.036	0.033	45
	$\dot{A}$, $\ddot{A}$, C_{rc3}, C_{rs3}	0.032	0.032	0.033	0.031	45
21	$\dot{A}$, C_{rc3}, C_{rs3}, $C_{\lambda c3}$,$C_{\lambda s3}$	0.019	0.019	0.020	0.018	45
	$\dot{n}$, C_{rc3}, C_{rs3}, $C_{\lambda c3}$,$C_{\lambda s3}$	0.018	0.019	0.019	0.017	45
22	$\dot{n}$, $\ddot{n}$, C_{rc3}, C_{rs3}, $C_{\lambda c3}$,$C_{\lambda s3}$	**0.016**	**0.015**	**0.016**	**0.016**	45

Therefore, parameters representing the radial and along-track direction variations should be added to the broadcast ephemeris design.

Some extra parameters are added to the basic broadcast ephemeris model to improve the fit accuracy. Many designs have been used to fit precise ephemerides, and the typical results of some designs are listed in Tables 3, 4, 5 and 6. After high-order rate parameters such as $\dot{A}$ and $\dot{n}$ are added, the fit accuracy of the radial and cross-track components improves significantly. Furthermore, third-order harmonic correction terms $\left(C_{rc3}, C_{rs3}, C_{\lambda c3}, C_{\lambda s3}\right)$ are also recommended. Thus, short-periodic variations can be represented more precisely.

According to the statistics of the fit errors shown in Tables 3, 4, 5 and 6, a 22-parameter model, i.e., the basic broadcast ephemeris model plus $\dot{n}$, $\ddot{n}$, C_{rc3}, C_{rs3}, $C_{\lambda c3}$, and $C_{\lambda s3}$, is proposed. Figure 1 shows the time series of fit errors for the 22-parameter model. For an arc length of 20 min,

Table 6 Results of fit errors in the radial (R), along-track (A), and cross-track (C) components and URE values with a 30 min arc length for the 800 km LEO satellite (unit: m)

No. Parameters	Extra parameters	URE RMS	R	A	C	Inclination (°)
16		18.664	18.717	18.886	18.405	45
17	$\dot{A}$	3.093	3.154	3.174	2.959	45
	$\dot{n}$	2.896	2.970	2.969	2.759	45
18	C_{rc3}, C_{rs3}	5.294	5.250	5.355	5.272	45
	$\dot{A}$, $\dot{n}$	2.655	2.766	2.739	2.472	45
	$\dot{A}$, $\ddot{A}$	1.622	1.651	1.632	1.588	45
	$\dot{n}$, $\ddot{n}$	0.371	0.374	0.390	0.349	45
19	$\dot{n}$, C_{rc3}, C_{rs3}	1.766	1.807	1.804	1.692	45
	$\dot{A}$, C_{rc3}, C_{rs3}	1.539	1.570	1.574	1.477	45
	$\dot{A}$, $\ddot{A}$,$\dot{n}$	0.442	0.459	0.451	0.418	45
	$\dot{A}$, $\dot{n}$,$\ddot{n}$	0.329	0.336	0.338	0.313	45
20	C_{rc3}, C_{rs3}, $C_{\lambda c3}$,$C_{\lambda s3}$	1.000	0.999	1.019	0.981	45
	$\dot{n}$, $\ddot{n}$, C_{rc3}, C_{rs3}	0.317	0.322	0.325	0.306	45
	$\dot{A}$, $\ddot{A}$, C_{rc3}, C_{rs3}	0.284	0.291	0.292	0.268	45
21	$\dot{A}$, C_{rc3}, C_{rs3}, $C_{\lambda c3}$,$C_{\lambda s3}$	0.137	0.139	0.139	0.134	45
	$\dot{n}$, C_{rc3}, C_{rs3}, $C_{\lambda c3}$,$C_{\lambda s3}$	0.132	0.134	0.133	0.129	45
22	$\dot{n}$, $\ddot{n}$, C_{rc3}, C_{rs3}, $C_{\lambda c3}$,$C_{\lambda s3}$	**0.080**	**0.085**	**0.081**	**0.075**	45

the fit errors in all three components remain within ± 5 cm, and the UREs are better than 4 cm. For an arc length of 30 min, the fit errors in the three components vary within ± 29 cm, and the UREs are better than 20 cm. The RMS values of the fit UREs for 20 and 30 min arc lengths are 0.012 and 0.058 m, respectively. The tables also show the relationship between the fit accuracy and arc length. As the arc length increases, the fit accuracy decreases dramatically. For 1000 km and 800 km orbits, after using the 22-parameter model, RMS values for fit UREs better than 10 cm can still be achieved within 20 min and 30 min arc lengths. The results in terms of the impact of arc length, orbital altitude, inclination, and eccentricity on the fit accuracy of our 22-parameter model and the model proposed by Xie et al. (2018) and Du et al. (2014) are compared. Because Du et al. (2014) designed broadcast ephemeris for GEOs, in this study, we add $\dot{n}$, C_{rc3}, C_{rs3}, $C_{\lambda c3}$, and $C_{\lambda s3}$ to the basic broadcast ephemeris model for higher accuracy.

Figure 2 shows the impact of inclination on fit UREs. The eccentricity and orbital altitude are still set as 0.001 and

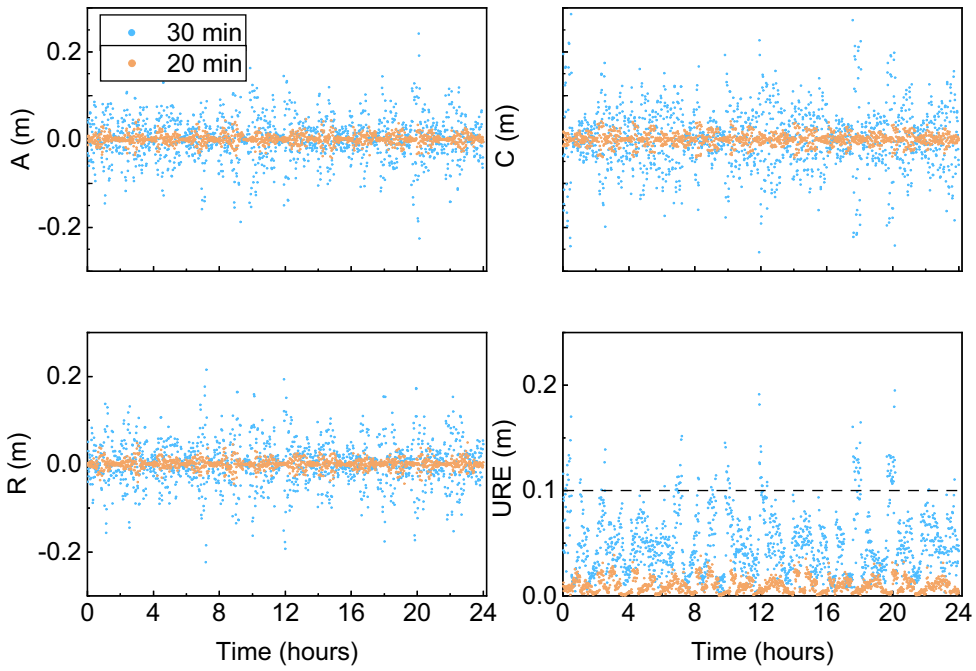

Fig. 1 Fit errors in the along-track (A), cross-track (C), and radial (R) components and the fit UREs with the 22-parameter model for the LEO satellite at 1000 km. The orange and blue points represent the fit errors of 20 and 30 min arc lengths for 24 h of precise ephemeris, respectively

1000 km, respectively, but the inclination varies from 0° to 90°. Thus, all values of inclination that may appear in the LEO constellation design are considered. Our 22-parameter model and the models proposed by Xie et al. (2018) and Du et al. (2014) are applied. The fit UREs remain stable as the inclination increases from 0° to 90° for our 22-parameter model. Therefore, the singularity caused by small eccentricity and small inclination can be overcome. Conversely, for the model proposed by Xie et al. (2018), the performance is the worst when the arc length is 20 min: in some cases, parameters cannot be generated because a singularity exists when the inclination is close to 0°.Because more high-order rate parameters are used, the performance of the Xie et al. (2014) model is slightly better when the arc length is longer. However, the fit accuracy is no better than 2.1 cm. This difference has a limited impact on positioning accuracy. When the inclination is larger, as a consequence of singularity problems, the model proposed by Du et al. (2014) cannot be generated. These singularity problems are due to the definition of the nonsingular elements used by Du et al. (2014) and Xie et al. (2018).

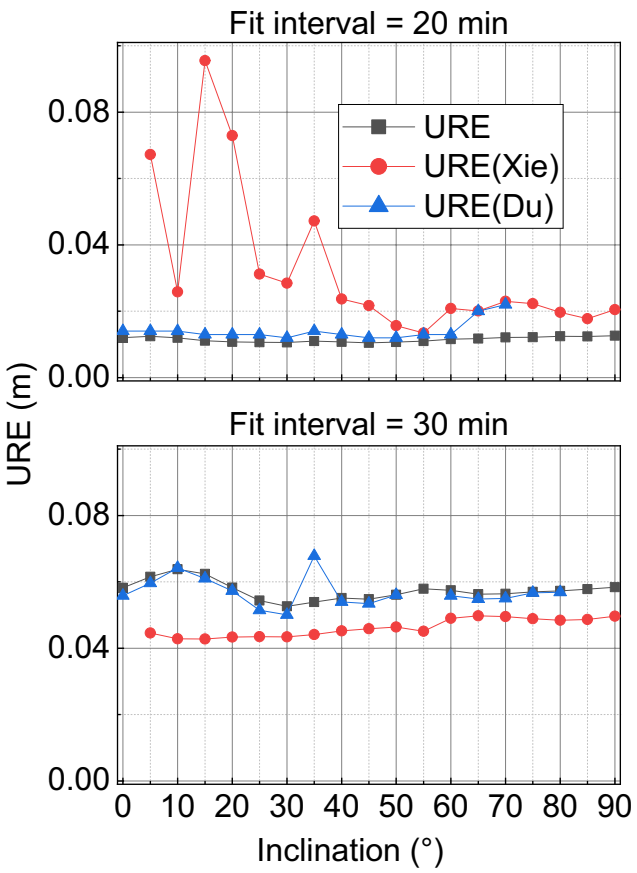

Fig. 2 Fit UREs of the 22-parameter model, and the models of Xie et al. (2018) and Du et al. (2014) as a function of the inclination (arc lengths: 20 min and 30 min). If there is no URE value, the parameters cannot be generated

Figure 3 shows the relationship between the fit UREs and eccentricity. The inclination and orbital altitude are set to 45° and 1000 km, respectively, and the eccentricity varies from 0.001 to 0.030. Our 22-parameter model outperforms the models of Xie et al. (2018) and Du et al. (2014). For our 22-parameter model, when the eccentricity is larger than 0.020, the fit accuracy decreases considerably. However, the eccentricities of LEO satellites are generally small, as are those of most GNSS satellites. The difference between the highest and lowest fit accuracies does not exceed 1 cm. Hence, in the future construction of LEO constellations, our 22-parameter model can satisfy the corresponding requirements in terms of eccentricity.

Figure 4 illustrates the effect of orbital altitude when inclination and eccentricity are set to 45° and 0.001, respectively. For the Du et al. (2014) model and our model, the fit accuracy improves considerably as the altitude increases. Our 22-parameter model again outperforms the models of Xie et al. (2018) and Du et al. (2014). As the orbital altitude increases, the perturbation forces become simpler, and the satellite operating states represented by 22 parameters are closer to reality. However, for Xie et al. (2014), simpler perturbation forces can potentially result in an overparameterization problem because more high-order rate parameters are included. Thus, when the orbital altitude is higher, the stability and fit UREs worsen; therefore, more parameters may not mean higher accuracy.

Validation of real LEO satellites

The experiments mentioned above are performed based on simulated precise ephemerides. Therefore, real LEO

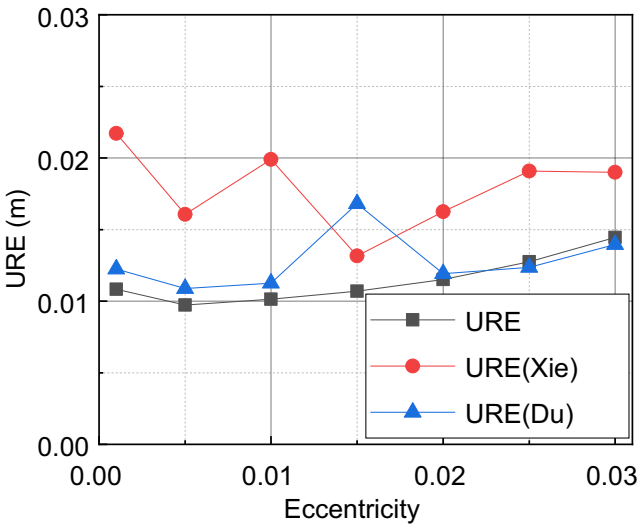

Fig. 3 Fit UREs of the 22-parameter model and the models of Xie et al. (2018) and Du et al. (2014) for LEOs of different eccentricities from 0.001 to 0.030 (arc length: 20 min)

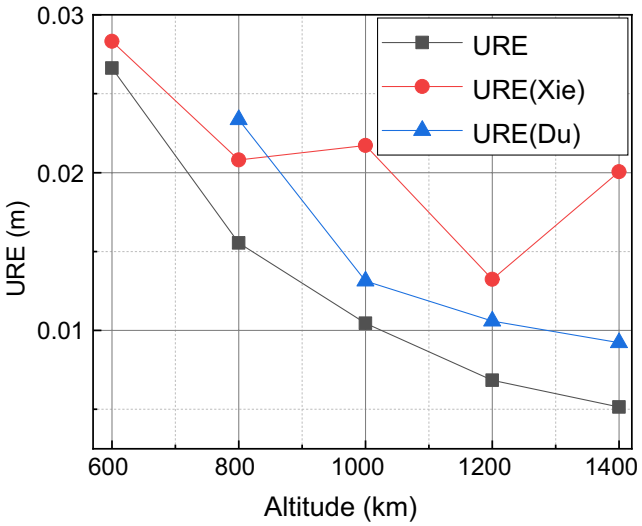

Fig. 4 Fit UREs of the 22-parameter model and the models of Xie et al. (2018) and Du et al. (2014) for LEO satellites at altitudes from 600–1400 km (arc length: 20 min). If there is no value, the parameters cannot be generated

satellites are used to validate our 22-parameter model. The real precise orbit products of these LEO satellites are used to generate broadcast parameters. Table 7 lists some basic orbit information of these satellites.

Figure 5 illustrates the RMS of the fit UREs for the four real LEO satellites. Similar to the results based on simulated precise ephemeris, the fit accuracy improves with higher orbital altitude. Although the eccentricities of these real satellites are close to zero, our 22-parameter model and the model of Xie et al. (2018) can still be successfully generated. However, due to the singularity caused by large inclinations, the parameters, except those for Jason-2, cannot be generated using the model proposed by Du et al. (2014). When the arc length is 20 min, the RMS values of the fit UREs for all LEO satellites do not exceed 10 cm. For a given orbital altitude, a shorter arc length results in higher fit accuracy. Figure 6 shows the fit URE time series of the HY-2A orbit for our 22-parameter model with 20 and 30 min arc lengths. When the arc length is 20 min, the fit accuracy is more stable and precise. For a 20 min arc length, the UREs are better than 6.5 cm; for a 30 min arc

Table 7 Basic orbit information of satellites used for broadcast ephemeris validation

Name	Inclination (°)	Eccentricity	Altitude (km)
GRACE-A	89	<0.005	500
CryoSat-2	92	0.000	720
HY-2A	99.35	0.00117	971
Jason-2	66	0.000	1300

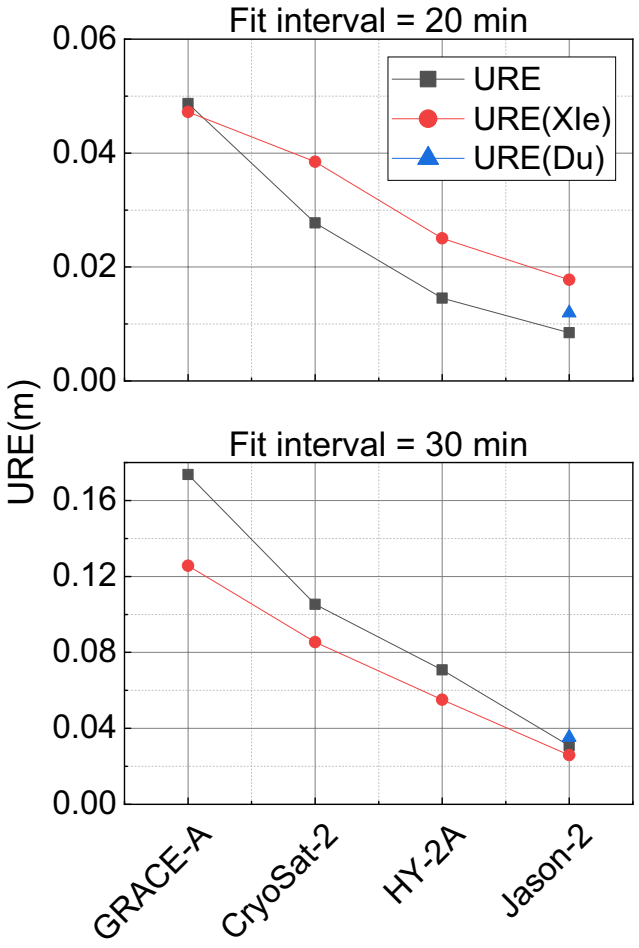

Fig. 5 Fit UREs of the 22-parameter model and the models of Xie et al. (2018) and Du et al. (2014) for real LEO satellites (arc lengths: 20 and 30 min). If there is no URE value, parameters cannot be generated

length, the UREs are better than 27 cm. The RMS values of the UREs for 20 and 30 min arc lengths are 1.5 and 7.1 cm, respectively. These results demonstrate that our improved nonsingular elements set is reliable.

Conclusions

Due to complex orbital variations, high-precision LEO satellite representation is difficult. We presented a model design of LEO broadcast ephemeris based on improved nonsingular orbital elements. In contrast to previous solutions, our model simultaneously eliminates singularities caused by small inclinations and eccentricities. To improve the fit accuracy, some additional parameters are included, and the fit errors are dramatically reduced.

The reliability of our proposed 22-parameter model is validated using both simulated and real satellites. The impact

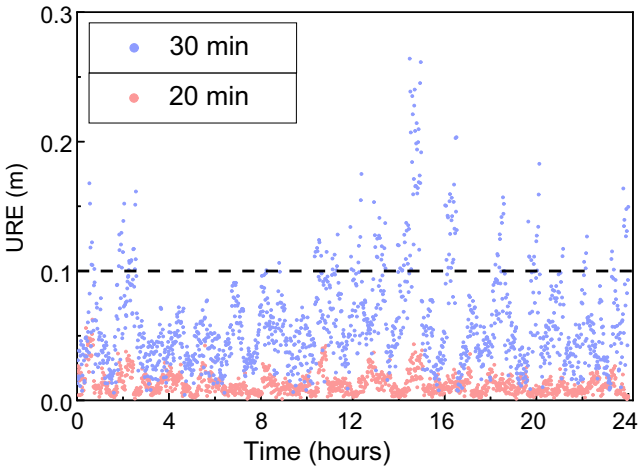

Fig. 6 Time series of fit UREs for the HY-2A satellite orbit for our 22-parameter model with 20 min and 30 min arc lengths. The red and blue points represent the fit UREs of 20 and 30 min arc lengths

of arc length, orbital altitude, eccentricity, and inclination is also discussed. The experimental results show that the fit UREs are dramatically reduced by an increase in orbital altitude and decrease in arc length. The fit UREs remain stable with variations in inclination, which means that singularities caused by small or large inclinations are removed simultaneously.

In this study, we focus on fit accuracy. Other factors, such as message block structure and interface design, are also critical for broadcast ephemerides design. These factors should be carefully analyzed in the future.

Acknowledgements This research is supported by the National Natural Science Foundation of China (No. 11673050); the Key Program of Special Development funds of Zhangjiang National Innovation Demonstration Zone (Grant No. ZJ2018-ZD-009); the National Key R&D Program of China (No. 2018YFB0504300); and the Key R&D Program of Guangdong province (No. 2018B030325001).

Data availability The simulated data are available upon request. And the real LEO satellites data can be downloaded in ftp.aiub.unibe.ch and ftp://doris.ign.fr

References

CSNO (2013) BeiDou navigation satellite system signal in space interface control document-open service signal, Version 2.0, 26, December 2013, China Satellite Navigation Office (CSNO) http://www.beidou.gov.cn/

Choi JH, Kim G, Lim DW, Park C (2020) Study on optimal broadcast ephemeris parameters for GEO/IGSO navigation satellites. Sensors 20(22):6544. https://doi.org/10.3390/s20226544

Department of Defense, U. S. A (2008) Global positioning system standard positioning service performance standard vol 35, https://www.gps.gov

Du L, Zhang Z, Zhang J, Liu L, Guo R, He F (2014) An 18-element GEO broadcast ephemeris based on non-singular elements. GPS Solut 19(1):49–59. https://doi.org/10.1007/s10291-014-0364-x

Enge P, Ferrell B, Bennett J, Whelan D, Gutt G, Lawrence D (2012) Orbital diversity for satellite navigation. In: Proceedings of the ION GNSS 2012, Institute of Navigation, Nashville, Tennessee, USA, September 12–21, pp 3834–3846

EU (2015) European GNSS (Galileo) open service signal in space interface control document. Issue 1.2, November 2015. European Union, https://galileognss.eu/

GPS Directorate (2013) Navstar GPS space segment/navigation user interfaces. Interface specification, IS-GPS-200H, Version H, September 23, 2013, Global Positioning Systems Directorate, https://www.gps.gov.

ICD-GLONASS (2016) Global navigation satellite system GLONASS, interface control document, general description of code division multiple access signal system. Edition 1.0, Russian Institute of Space Device Engineering, https://glonass-iac.ru

Joerger M, Gratton L, Pervan B, Cohen CE (2010) Analysis of iridium- augmented GPS for floating carrier phase positioning. Navigation 57(2):137–160

Li B, Ge H, Ge M, Nie L, Shen Y, Schuh H (2019a) LEO enhanced global navigation satellite system (LeGNSS) for real-time precise positioning services. Adv Space Res 63(1):73–93. https://doi.org/10.1016/j.asr.2018.08.017

Li X, Ge M, Dai X, Ren X, Fritsche M, Wickert J, Schuh H (2015) Accuracy and reliability of multi-GNSS real-time precise positioning: GPS GLONASS, BeiDou, and Galileo. J Geod 89(6):607–635. https://doi.org/10.1007/s00190-015-0802-8

Li X, Ma F, Li X, Lv H, Bian L, Jiang Z, Zhang X (2019b) LEO constellation-augmented multi-GNSS for rapid PPP convergence. J Geod 93(5):749–764. https://doi.org/10.1007/s00190-018-1195-2

Ma FJ, Zhang XH, Li XX, Cheng JL, Guo F, Hu JH, Pan L (2020) Hybrid constellation design using a genetic algorithm for a LEO-based navigation augmentation system. GPS Solut 24(2):62. https://doi.org/10.1007/s10291-020-00977-0

Montenbruck O, Gill E (2000) Satellite orbits, models, methods and applications. Springer, Berlin. https://doi.org/10.1007/978-3-642-58351-3

Montenbruck O, Steigenberger P, Hauschild A (2015) Broadcast versus precise ephemerides: a multi-GNSS perspective. GPS Solut 19(2):321–333. https://doi.org/10.1007/s10291-014-0390-8

Reid TG, Neish AM, Walter TF, Enge PK (2016) Leveraging Commercial Broadband LEO Constellations for Navigating. In: ION GNSS 2016, Institute of Navigation, Portland, Oregon, USA, September 12–16, 2300–2314

Ruan R, Jia X, Wu X (2011) Broadcast ephemeris parameters fitting for GEO satellites based on coordinate transformation. Acta Geodaetica et Cartographica Sinic 40(Sup):145–150

Steigenberger P, Montenbruck O, Hessels U (2015) Performance evaluation of the early CNAV navigation message. Navigation 62(3):219–228. https://doi.org/10.1002/navi.111

Wang A, Chen J, Zhang Y, Wang J, Wang B (2019) Performance evaluation of the CNAV broadcast ephemeris. J Navig 72(5):1331–1344. https://doi.org/10.1017/s037346331900016x

Wang J, Wang J (2014) Fitting and extrapolating accuracy of GPS broadcast ephemeris. J Liaon Technic Univ (Nat Sci) 33(8):1118–1122

Xie X, Geng T, Zhao Q, Liu X, Zhang Q, Liu J (2018) Design and validation of broadcast ephemeris for low Earth orbit satellites. GPS Solut 22(2):54. https://doi.org/10.1007/s10291-018-0719-9

Yin H, Morton YT, Carroll M, Vinande E (2015) Performance analysis of L2 and L5 CNAV broadcast ephemeris for orbit calculation. Navigation 62(2):121–130

Lingdong Meng is currently a Ph.D. candidate at the College of Surveying and Geo-Informatics, Tongji University, China. His current research areas include multi-frequency GNSS data processing and the Low Earth Orbit (LEO) satellite constellation enhanced GNSS navigation and positioning.

Junping Chen is a Professor and the head of the GNSS data analysis group at Shanghai Astronomical Observatory (SHAO). He received his Ph.D. degree in Satellite Geodesy from Tongji University in 2007. Since 2011, he has been supported by the "one hundred talents" programs of the Chinese Academy of Sciences. His research interests include multi-GNSS data analysis and GNSS augmentation systems.

Jiexian Wang obtained his Ph.D. degree from Shanghai Astronomical Observatory (SHAO), Chinese Academy of Sciences and has been working at Tongji University for 32 years, where he is currently a professor. His main research interest is in the study of GNSS positioning and its applications.

Yize Zhang is currently an associate professor at Shanghai Astronomical Observatory (SHAO). He received his Ph.D. degree from Tongji University in 2017. Then, he did his postdoctoral researcher at the Tokyo University of Marine Science and Technology (TUMSAT). His current research mainly focuses on multi-GNSS precise positioning and GNSS biases analysis.